Cell Communication and Adhesion, 10: 69–83, 2003

ISSN: 1541-9061 print / 1543-5180 online
DOI: 10.1080/15419060390260987

Taylor & Francis
healthsciences

Focal Contact Clustering in Osteoblastic Cells under Mechanical Stresses: Microgravity and Cyclic Deformation

ALAIN GUIGNANDON[1], OMAR AKHOUAYRI[1], YVES USSON[2], ALINE RATTNER[1], NORBERT LAROCHE[1], MARIE-HÉLÈNE LAFAGE-PROUST[1], CHRISTIAN ALEXANDRE[1], and LAURENCE VICO[1]

[1]*Laboratoire de Biologie du Tissu Osseux (L.B.T.O.), Institut National de la Santé et de la Recherche Médicale (INSERM), Saint Etienne, France and*

[2]*Laboratoire TIMC, UMR 5525 CNRS, RFMQ Team, Institut Albert Bonniot, Université Joseph Fourier, Domaine de la Merci, La Tronche, France*

We quantitatively compared vinculin-related adhesion parameters in osteoblastic cells submitted to two opposing mechanical stresses: low deformation and frequency strain regimens (stretch conditions) and microgravity exposure (relaxed conditions). In both ROS 17/2.8 cells and rat primary osteoblastic cells, 1% cyclic deformations at 0.05 Hz for 10 min per day for seven days stimulated cell growth compared to static culture conditions, while relaxed ROS cells proliferated in a similar way to static cultures (BC). We studied the short-term (up to 24 h) adaptation of focal contact reorganization under these two conditions. Cyclic deformation induced a biphasic response comprising the formation of new focal contacts followed by clustering of these focal contacts in both ROS cells and primary osteoblasts. Microgravity exposure induced a reduction in focal contact number and clustering in ROS cells. To evaluate whether the proliferation (stretch) or survival (relaxed) status of ROS cells influences focal contact organization, we inhibited the ERK proliferative-dependent pathway. Inhibition of proliferation by PD98059 was partially reversed, but not fully restored by stretch. Stretch-induced clustering of vinculin-positive contacts also persisted in the presence of PD98059, whereas the increase in focal contact number was abolished. In conclusion, we show that focal contacts are mechanoeffectors, and we suggest that their morphologic organization might serve as a discriminant functional parameter between survival and proliferation status in ROS 17/2.8 osteoblastic cells.

Keywords. Confocal microscopy, cytoskeleton, image analysis, mechanical stress, microgravity, osteoblasts, vinculin

INTRODUCTION

Cyclic loads are able to increase bone mass by stimulating bone formation. In contrast, reduction of mechanical stimulation, as encountered under microgravity conditions during space flight, induces osteopenia (40). Mechanical stimulation is more efficient when the osteogenic loading regimen is able to increase osteoblast recruitment (24). Osteoblastic cells respond to mechanical strain by altering their proliferation, protein synthesis, and possibly their matrix mineralization (2, 4). However, contrary to other cell types, there is a substantial lack of information concerning the mechanisms by

Received 10 December 2002; accepted 19 May 2003.
Address correspondence to Laurence Vico, LBTO, INSERM E366 Faculté de Médecine, 15, rue Ambroise Paré, 42023, St Etienne Cedex 02, France. E-mail: vico@univ-st-etienne.fr

which cells of the osteoblastic lineage perceive and translate mechanical signals into biochemical signal cascades (i.e., mechanotransduction), which consequently lead to alteration in cell growth or other functions.

There is some evidence to suggest that integrins act as mechanotransducers in several cell types including osteoblasts (3, 19, 26). Cell-matrix interactions occur at the closest contacts between the cell and the substratum: focal adhesion. They are formed by a complex network of cytoskeletal proteins that links the filamentous actin (F-actin) cytoskeletal network via integrins to the extracellular matrix (ECM) (12, 27, 31). Integrins have long been recognized for their structural roles in regulating cell shape, cell migration, and tissue architecture. More recently, it has become clear that integrin receptors can initiate intracellular signals that act synergistically with those from growth-factor receptor protein-tyrosine kinases in modulating cell growth. More knowledge has recently been acquired concerning integrin-stimulated tyrosine phosphorylation events and downstream signaling pathways, mainly mitogen-activated protein (MAP) kinase cascades (see 5 and 33 for review). Activation of MAPK pathways has been demonstrated to increase transcription of the cyclin D1 gene, the growth factor responsive cyclin important for cell cycle progression (16). Mechanical signals have also been shown to activate MAPK pathways in pulmonary epithelial cells (7), smooth muscle cells (45), and endothelial cells (36).

We have previously demonstrated that cell proliferation in ROS 17/2.8 cells was simply maintained during a 6-day microgravity mission (9), but was increased under stretch conditions (this study). We have also recently demonstrated that integrin-mediated organization and cytoskeleton integrity are specifically modified as a function of cell cycling during microgravity exposure (10). Briefly, after four days of flight, post-mitotic cells presented a marked reduction in cell area, vinculin-positive contact number, and mean area (clusterization) compared to non-mitotic cells, suggesting that long-term adaptation under relaxed mechanical conditions leads to the formation of immature focal contacts.

Our working hypothesis was based on the fact that mechanical stress is able to stimulate cell proliferation, and that lack of stress, such as during microgravity exposure, did not and thus dramatically reduced focal adhesion. We hypothesized that the organization of focal adhesion is regulated by mechanical stresses and could be related to the proliferation status of cells.

The mechanical signal can be more easily manipulated and cellular focal contact adaptation can be more easily studied with the FlexerCell® apparatus than by microgravity experiments. We first defined a mechanical regimen able to increase proliferation in ROS cells and primary osteoblasts. We then analyzed the kinetic changes of a potential mechanotransducer, the vinculin-positive focal contact, over the first 24 hours of strain application. Vinculin was selected as a representative of focal contact, as it is one of the last proteins that colocalize to the integrin cluster and it does so only after integrins have bound to the extracellular matrix (20). We deliberately applied a low amplitude and low frequency range strain regimen compared to that usually reported in the literature (23, 37, 38) in order to approximate physiological tissue levels. We first compared adhesion changes obtained under these conditions with those observed after 12 and 24 hours of microgravity exposure. In a second step, the kinetic changes of focal adhesion in the presence of an MAP kinase inhibitor, known to significantly reduce cell proliferation, were quantified. A previously published approach for quantification of focal contact-associated proteins (high-resolution confocal acquisition and image analysis) was used (39).

Focal contact formation or release are dependent on integrity of the cytoskeletal network. It is clear that the formation of focal contacts depends on the actin-myosin machinery that generates tension (21). Conversely, the release of focal contacts depends on the function of microtubules that tagged the contact before dissociation (13). Cytoskeletal adaptation of ROS cells in response to these mechanical stresses was appraised by visualization of F-actin, vimentin and microtubule structures. Focal contact turnover is related to cytoskeletal dynamics, regulated by

tension forces of microfilaments and opposing compression forces of microtubules (41).

MATERIALS AND METHODS

Cell Culture

- **Cell Line**
  Osteosarcoma ROS 17/2.8 cells derived from Wistar rats (22) are well defined cells, presenting the same characteristics as mature osteoblasts (alkaline phosphatase and osteocalcin expressions and ability to mineralize the extracellular matrix). They were also chosen because they present large and well delimited focal contacts (Figure 1A) allowing high resolution image analysis.
  These cells were maintained in tissue culture T75-flasks (Elvetec Services, Venissieux, France) in Dulbecco's Modified Eagle's Medium (DMEM, Boehringer, Gagny, France) supplemented with 10% fetal bovine serum (FBS, Boehringer, Gagny, France), 2 mM L-glutamine and 1% antibiotics (10,000 U of penicillin and 10 mg of streptomycin, Sigma, St. Quentin Fallavier, France). Cultures were incubated in a humidified atmosphere of 5% CO_2 at 37°C (Incubator Queue, France). At confluence, cells were trypsinized with 1× trypsin-EDTA (Sigma, France) and were seeded on 35 mm type I collagen bottomed-flexible wells (BioFlex® at a density of 10^5 cells/well.
  To assess proliferation and morphological analysis of focal contact and cytoskeleton, ROS 17/2.8 cells were grown in 10% FBS, (Figures 1, 2, 3, and 4). In experiments with MEK inhibitor (PD-98059), presented in Figure 5, 50 μM of PD-98059 (Merck EuroLab, SA, FRANCE) was added to serum-free cell culture medium replacing the 10% FBS medium two hours before strain application. Cells were then starved of serum for 26 hours. In Figure 2C, PD-98059 was added in 10% FBS and the 10% FBS-PD98059 medium was changed every day.

- **Primary Cells**
  Primary cells were obtained from enzymatic digestion of the femoral metaphysis of two male Wistar rats (three weeks old). After removing soft tissues, metaphyses were reduced to approximately 2-mm-wide fragments and then submitted to three sequential 10-minute digestions with 1 mg/ml of *Clostridium histolyticum* neutral collagenase (Sigma, France) in medium at 37°C with stirring. The cell suspension was then removed, neutralized with medium supplemented with 15% FBS, centrifuged at 1300 rpm for five minutes and resuspended in medium supplemented with 10% FCS, 50 μg/ml ascorbic acid, 2 mg/ml ß-glycerolphosphate and 10^{-8}M dexamethasone. The medium was changed after the first 24 hours to remove nonadherent cells. Subsequently, medium was changed every other day. Cultures were maintained in a humidified atmosphere of 95% air with 5% CO_2 at 37°C. After five days, the primary cells were passaged using 1× collagenase-trypsin-EDTA and seeded on 35 type I collagen bottomed-flexible wells at a density of 10^5 cells/well.
  Both ROS 17/2.8 and primary cells were seeded 72 hours before strain application to ensure that they were well attached to the matrix that they had produced.

Application of Deformation to Cultures

The FX-3000® Flexercell Strain unit (Flexcell International Corp.®, Hillsbough, USA) was used to apply mechanical strain to osteoblasts. The unit is designed to exert controlled strain on cultured cells, (i.e., frequency, amplitude, and duration of strain controlled by a computer). The instrument is composed of an FX-3000 FlexCentral system controller, an SVGA color monitor, a keyboard and serial mouse, and Flexercell vacuum Bioflex® baseplate and gaskets on which the culture plates were placed in a CO_2 incubator. The Bioflex® baseplate contains the Bioflex® loading stations consisting of six

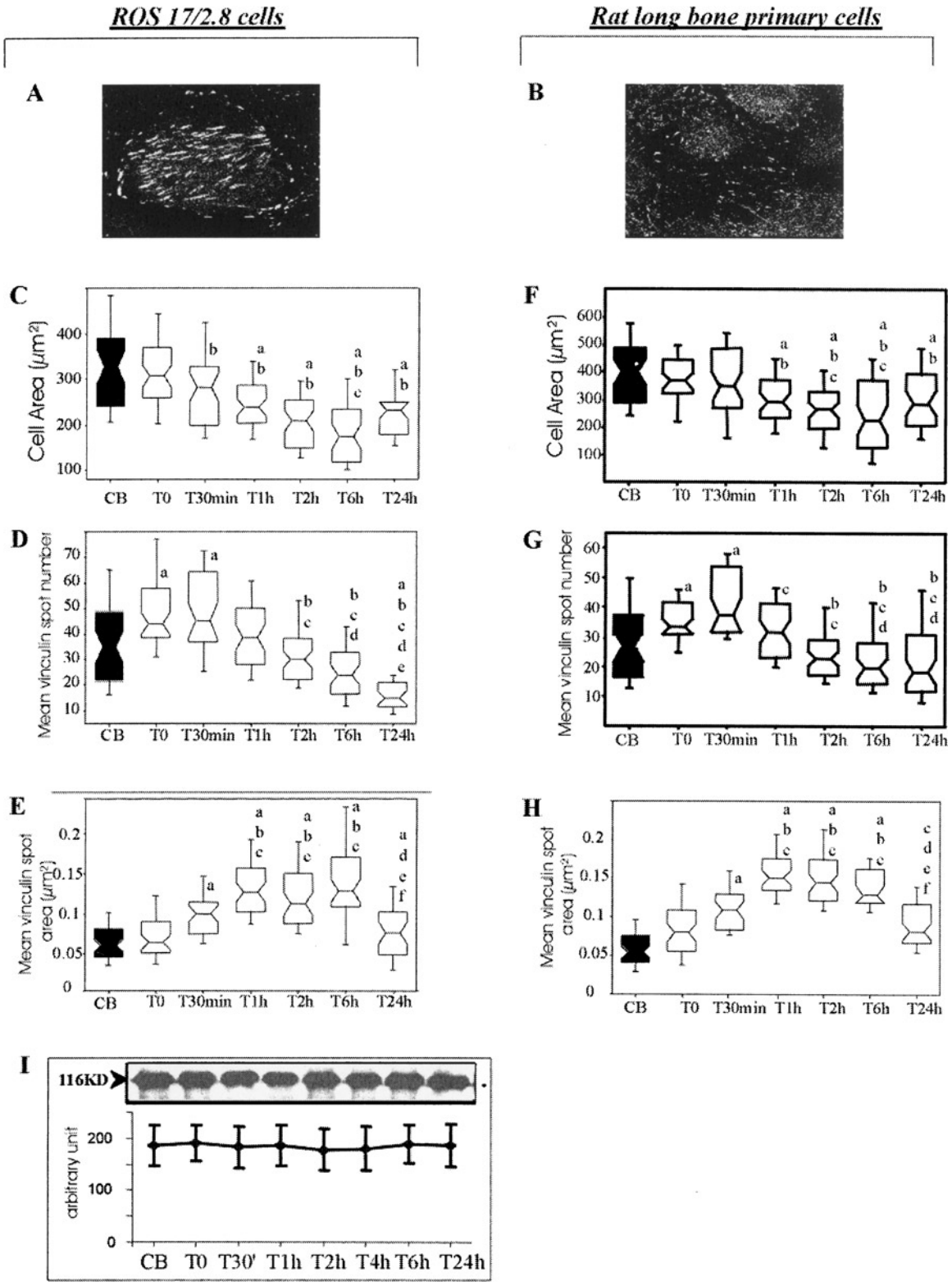
ROS 17/2.8 cells
Rat long bone primary cells
A
B
C
F
D
G
E
H
I
Cell Area (µm²)
Mean vinculin spot number
Mean vinculin spot area (µm²)
CB T0 T30min T1h T2h T6h T24h
116KD
arbitrary unit
CB T0 T30' T1h T2h T4h T6h T24h

buttons per plate that insert into each plate allowing uniform magnitude of strain on 85% of the surface of the flexible wells. Cells subjected to stretch were grown on specially designed six-well tissue culture dishes with flexible silicone bottoms. A negative pressure was applied by an air pump to the flexible bottomed wells at three cycles per minute (0.05 Hz) for 10 minutes each day. During each cycle, a 10-second strain period was followed by a 10-second relaxation period (duty cycle 50%). As the flexible bottoms are pulled downward by the negative pressure, the cells attached to their upper surface are strained by the deformation of the rubber. The experimental protocols used in this study delivered a 0.3% (3000 μStrain) to 2% (20000 μStrain) elongation. A strain value of 0.3% is the lowest strain value that can be reliably and reproducibly delivered by the Flexcell.

Microgravity Experiment

Foton 12 space flight experiments were carried out on the Russian Foton unmanned recoverable capsules. Capsules were launched into polar orbits by Soyuz vehicles from the Plesetsk base (650 km to the north of Moscow). Capsules flew through space for 15 days. They then left microgravity to return to Earth and landed in Kazakhstan, south of Samara.

Ibis Incubators developed by CNES (*Centre National d'Etudes Spatiales* [French Space Agency]) provided the following culture conditions: 37°C, absence of CO_2 exchange, possibility of injecting products into the medium during the flight, sample fixation, and inflight centrifuge (C) generating 1g and acting as a control with inflight static culture (flight μg: F). Centrifuge and flight cultures experienced the same vibrations, mainly due to take-off. The 1g centrifuge was used as the in-flight unit-gravity reference. Static ground cultures at 1g were also maintained as controls to test the effects of space flight conditions. After landing of the capsules, the fixed cell cultures were stored at 4°C during transportation and directly processed for immunohistochemistry on arrival at the laboratory. We have previously established, in ground experiments, that antigenic sites are not altered by storing fixed samples at 20°C for 10 days. The experiment was prepared at the Plessetsk launch base (Russia). ROS 17/2.8 cells were plated three days before launch at 5×10^3 cells/cm^2 on glass coverslips (Nunc, Life Technologies) to ensure that they were well attached to their own matrix. The culture chamber consisted of a single bag (2 ml) containing the glass coverslip (2 cm^2) and two compartments, one containing serum and the other containing fixative (4% paraformaldehyde solution). These liquids can be delivered into the culture compartment according to the preprogrammed activation time line.

Determination of Cell Number

Once cells were released from their culture substratum, their number was determined at various time points by direct counting with a hemocytometer. At each time point, cell number was counted four times using the trypan blue dye exclusion method to assess cell viability. In microgravity experiments, the number of cells was determined by the number of cells per field of images analyzed for quantification of focal contacts. Using this method, we obtained similar results to those observed during the Bion 10 mission, based on colorimetric (methylene blue) methods (9). Results were expressed as the percentage of baseline control.

Figure 1. Comparative analysis of vinculin-positive focal contacts in ROS 17/2.8 cells and rat primary osteoblasts. ROS 17/2.8 cells and rat primary cells were strained during a single 10-min period, at 1%, 0.05 Hz. They were then fixed at different time points during the recovery period. (A–B). Characteristic pattern of vinculin-positive focal contacts in (A) ROS 17/2.8 and (B) rat primary cells. (C–D) Cell area, mean vinculin spot number/cell, and Mean vinculin spot area analyzed in ROS 17/2.8 cells. (F-H) Cell area, mean vinculin spot number/cell, and Mean vinculin spot area analyzed in rat primary cells. Black boxes represent control unstrained cells; empty boxes, strained cells. Values are the median (25th to 75th percentiles). (I) Western blot of vinculin protein in ROS 17/2.8 cells sampled throughout the recovery period. Significant differences at $p < 0.05$ are: a: vs. control; b: vs. T0; c: vs. T30min; d: vs. T1h; e: vs. T2h; f: vs. T6h.

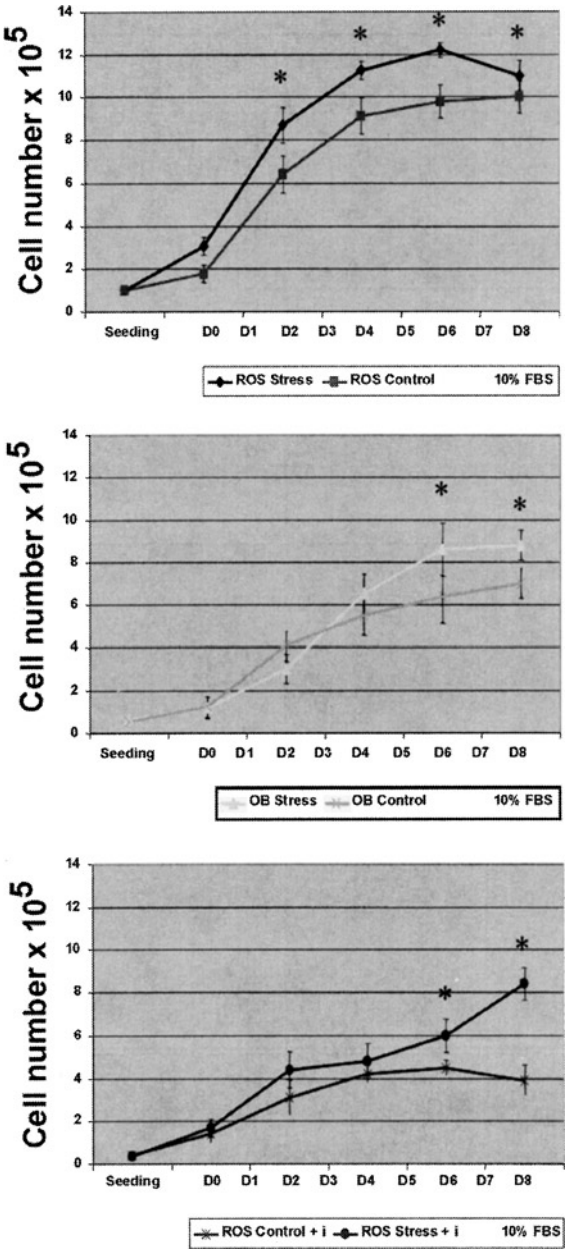

Figure 2. Cell growth of strained osteoblastic cells. Cell proliferation evaluated under standard culture conditions (10% FBS). Values are means ± SD of six determinations. Cells were seeded three days before application of the strain. ROS 17/2.8 cells (top), rat long bone primary cells (middle) and ERK inhibitor treated ROS cells (bottom) were strained for 10 min per day from day 0 to day 8, at 1% and at 0.05 Hz. ERK inhibitor was added in 10% FBS two hours before strain application and the 10% FBS-PD98059 medium was changed every day. Cells from the strain regimens were significantly more numerous ($p < 0.05$), than those from static control conditions at the same time point.

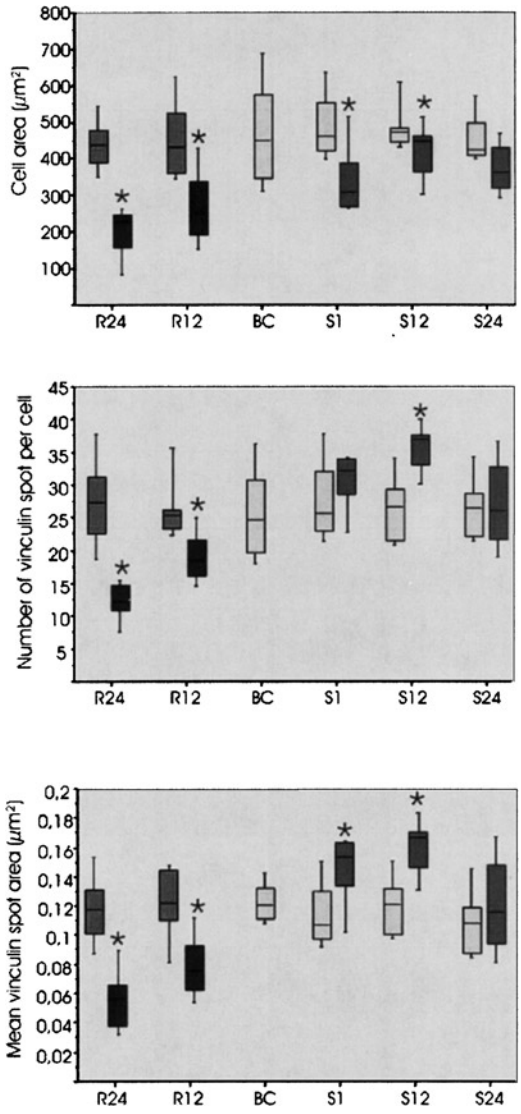

Figure 3. Quantification of vinculin-positive focal contacts in strained and relaxed ROS 17/2.8 cells. From top to bottom: Cell area in μm^2, mean number of vinculin spots per cell (VN), and mean vinculin spot area per cell in μm^2 (VA). Values are medians (20th to 80th percentiles). Yellow boxes represent static controls cultured on type I collagen-coated silicone membranes; BC represents baseline control cultured on glass; green boxes represent the 1 g inflight centrifuge controls cultured on glass; blue boxes represent the microgravity relaxed (R) conditions cultured on glass; and red boxes represent the strained cells (S) cultured on type I collagen-coated silicone membranes. BC represents the baseline control of the experiment under static culture conditions on glass coverslips. Centrifuge and Static conditions were the appropriate controls for relaxed and stretch conditions, respectively. Note that, despite the difference in substratum for static cells and BC, we found similar ranges of values for cell area, VN, and VA. Significant difference ($p < 0.01$) from static or centrifuge controls at the same time point.

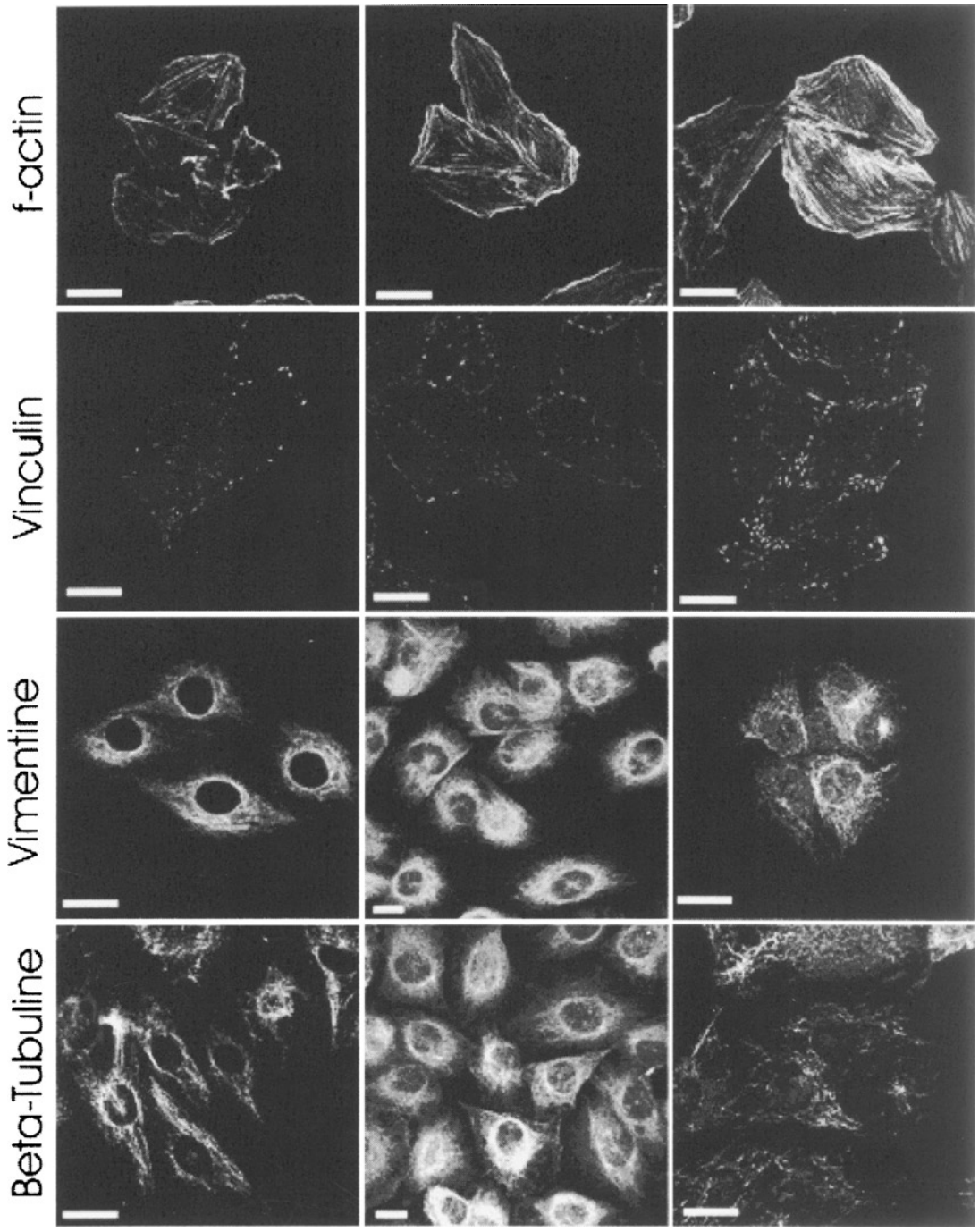

Figure 4. ROS 17/2.8 cytoskeleton integrity under relaxed, static, and strained conditions. Representative images of fibrous actin, vinculin, vimentin, and beta-tubulin obtained on ROS 17/2.8 cells submitted to microgravity conditions (left column), static control culture (center), and strained conditions (right column). Bars represent 20 μm. Marked differences were observed between BC and relaxed conditions and BC and strained conditions for F-actin and between BC and strained conditions for beta-tubulin. Also note that it is difficult to draw any conclusions about vimentin structures due to the lack of difference between strained, static, and relaxed images. See Figure 1 for quantification of vinculin staining.

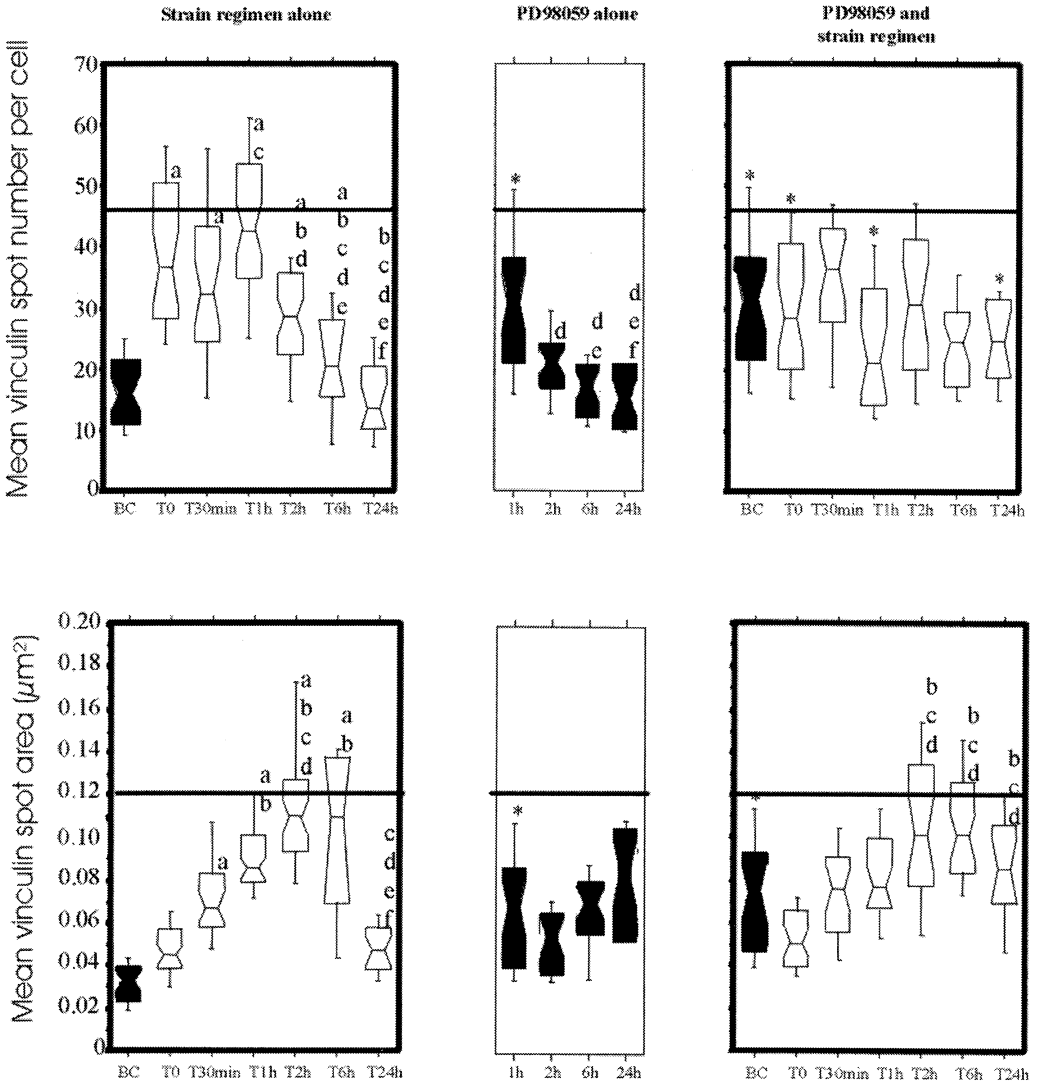

Figure 5. Quantification of vinculin-positive focal contacts and ERK1/2 signaling. Results of image analysis and quantification of mean vinculin spot number (top line) and mean vinculin spot area (bottom line) in strained ROS 17/2.8 cells (left column), 50 μM PD98059 treated ROS 17/2.8 cells (middle column), or PD98059 treatment combined with strain regimen (right column). Cells were strained during a single 10-min period, at 1%, 0.05 Hz. Black boxes represent control unstrained cells; empty boxes represent strained cells during recovery period. Values are the median (25th to 75th percentiles). Significant differences at $p < 0.01$ are: *: vs. BC of strain regimen alone; a: vs. BC; b: vs. T0; c: vs. T30min; d: vs. T1h; e: vs. T2h; f: vs. T6h.

Immunostaining

Cells were washed in PBS and fixed with 4% paraformaldehyde at room temperature for 10 minutes and permeabilized by 0.1% triton X-100. Nonspecific binding was blocked by 1% Bovine Serum Albumin (BSA) in PBS. Primary antibodies (monoclonal antihuman vinculin clone hVIN-1, monoclonal anti-vimentin-Cy3, anti-beta-tubulin-Cy3 and FITC conjugated IgG were purchased from Sigma, St. Quentin Fallavier, France. Cells were then incubated with appropriate antibodies in PBS overnight at 4°C. The specimens were washed in PBS containing 0.5% BSA and incubated

with a fluorescein isothiocyanate (FITC)-conjugated IgG. F-actin was stained using BODIPY-FL phallacidin (B-607 Molecular Probes, Leiden, Netherlands). Cells were extensively washed with 0.5% BSA in PBS and mounted in Fluoprep (BioMérieux SA, France).

Confocal Microscopic Acquisition

Vinculin immunostaining was observed with a LSM410 confocal microscopy system (Carl Zeiss, Iena, Germany). FITC fluorescence was excited with the 488 nm line of an air-cooled Argon laser. The emission light was separated from the excitation light by a 510 nm dichroic beam splitter. A 510–560 nm bandpass filter was then used to select the specific fluorescence emission of FITC. One confocal section per cell was recorded with the focus set inside the cell, 0.55 μm from the interface between the cell membrane and silicone thresholding. Eight images were averaged in order to improve signal-to-noise ratio. The images were coded over a 256-level gray scale.

Image Analysis

Cells were analyzed with a semiautomatic image analyzer (SAMBA-Alcatel®) with about 120 cells per condition. Quantification was performed on confocal scanning laser images of vinculin staining and was based on thresholding of vinculin adhesion plaques (details are reported in 20). Image processing allowed the calculation of 12 parameters describing morphologic and topographic parameters of focal contacts (20). Briefly, they included the cell area (CA), the cell shape factor, the mean vinculin spot area or number, and the spot shape factor.

Three topographic features were also calculated in order to express the spatial organization of the fluorescent spots within the cell (either peripheral or central) as well as their orientation.

Western Blot

ROS 17/2.8 cells on Bioflex wells were lysed in 0.5 ml of Tris-buffered saline containing 1% Triton X-100, 1% deoxycholate, and 0.5% SDS (Sigma, France). Cells were scraped from the substrate after 5 min in lysis buffer, and the insoluble material was removed by centrifugation. The supernatant was transferred to a new tube, and the protein concentration was determined using Bradford's method (2). Ten μg samples were loaded onto 7.5% SDS-PAGE gels for separation and transferred to nitrocellulose for immunoblot analysis. The nitrocellulose was blocked with 2% (w/v) dried skimmed milk proteins, washed, and then incubated with specific antivinculin antibodies overnight at 4°C. Blots were detected with biotinylated antimouse antibody, horseradish peroxidase-conjugated streptavidin, ECL reagents (BioSys, France), and Hyper ECL film (Perce, France). Bands intensities were determined by densitometry using Scion Image program (Scion corporation, Suite H, Maryland).

Statistical Analysis

For image analysis, 100 to 150 cells were analyzed at each time point and for each condition. Multivariate analysis tools were used to discriminate groups and to assess the significance of measurements (or variables). Initially, all data were pooled and the correlation matrix was calculated. Factorial discriminant analysis is a multivariate statistical analysis designed to emphasize the differences between experimental groups, based on measurements of several parameters (18). Comparisons between groups were based on the most discriminant parameters using the Friedman test. When the Friedman test was significant, the Mann-Whitney test was used to compare Flight versus Centrifuge or Strained versus Controls at 12 or 24 h (with an α-level $\approx$ [nominal α] $\times$ [number of comparisons made].

For kinetic analysis of stretched cells (0 to 24 h), comparisons between each time point were performed with ANOVA and post hoc tests ($p < 0.01$).

RESULTS

Cyclic Loads with Low Magnitude and Low Frequency were Osteogenic for ROS 17/2.8 and Primary Osteoblasts

The choice of strain regimen was based on the capacity of mechanical stimulation to induce osteoblastic proliferation. Figure 2 shows ROS 17/2.8 cell number under strained conditions versus unstrained controls. We investigated several regimens at low frequency and amplitude ranges. The low frequency ranges minimized culture medium shear stress allowing us to analyze the effect of substrate deformation. The growth pattern was similar between the various mechanical cyclic strain regimens (0.3%, 0.5%, 1%, and 2% at 0.05 Hz, data not shown). An increased growth pattern was also observed with rat primary cells at 1%, 0.05 Hz (Figure 2). In the control experiment, we added PD98059 and, as expected, cell growth was dramatically reduced compared to noninhibited cells. Under cyclic strain conditions, and despite the presence of inhibitor, the number of cells was significantly enhanced compared to the corresponding controls, especially after day 6 and day 8. At day 8, the difference of proliferation between inhibited strained and unstrained cells was even greater than under conditions without PD98059.

Strain and Relaxed Conditions Induced Opposite Focal Contact Reorganization

Three discriminant parameters were identified by factorial discriminant analysis: cell area (CA), mean vinculin spot number per cell (VN), and mean vinculin spot area (VA). Figure 3 illustrates the comparison between static conditions and stretch conditions (S) (red) as a function of time (1, 12, and 24 hours) for each of these parameters. Stressed cells presented a significant reduction of CA, regardless of the level or frequency of stimulation. Comparison of VN and VA showed that stretched and relaxed conditions induced opposing types of focal contact organization. Stretch induced new focal contact formation (+50% increase of mean vinculin spot number per cell at S12) and induced clustering around vinculin-positive contacts (+50%) after 1 and 12 hours. Control groups (i.e., BC & centrifuge) expressed almost the same values for CA, VN, and VA. In microgravity experiments, after 12 or 24 hours of flight exposure, ROS cells presented a marked reduction in VN and VA (about—100%). The values of CA, VN, and VA of strained cells returned to baseline control values 24 hours after application of the mechanical regimen, suggesting that after a 10-minute cyclic load, ROS cells rapidly changed their focal contact organization.

Kinetics of Focal Contact Organization in the Osteoblastic Cell Line and Primary Cells

In a complementary experiment, the kinetics of focal adhesion changes were studied first ROS 17/2.8 cells, in the presence of 10% FBS, during recovery after various regimens (10 min, 0.3%, 0.5%, 1%, or 2% at 0.05 Hz). Cells were fixed at T0, corresponding to the end of strain, or after 30 min (T30min), 1 h (T1h), 2 h (T2h), 6 h (T6h), and 24 h (T24h). Figure 1 illustrates the variations of these parameters obtained after a 1% deformation as a function of time in ROS 17/2.8 cells and rat long bone primary cells. In ROS 17/2.8 cells, CA (Figure 1C) was reduced compared to control cells, mainly between T1h and T6h. Strained cells (Figure 1D) adapted by an immediate increase in VN (30% vs. control at T0), and followed by a decrease from T2h to T24h. At about the same time, VA increased and remained elevated between T1h and T6h and returned to T0 baseline values by T24h (Figure 1E). Importantly, we observed the same kinetics of events for CA, VN, and VA in ROS 17/2.8 serum-starved cells (Figure 5). We also observed a similar profile in the other strain conditions (0.3%, 0.5%, and 2% at 0.05 Hz), except that, at 0.3% and 0.5%, VN and VA recovery was complete by 24 h (data not shown).

Western blot analysis (Figure 1I) showed no variation of total vinculin protein at any time point,

indicating that VA and VN alterations were not due to *de novo* vinculin synthesis, but to redistribution of protein among focal contacts. The kinetics of vinculin-positive focal adhesion changes were then studied in rat primary cells during recovery after a 10-minute 1%, 0.05 Hz strain regimen. Similar significant time-related changes to those observed in ROS 17/2.8 cells were demonstrated for CA, VN, and VA, except that the amplitude changes were less pronounced in primary cells than in ROS 17/2.8 cells (about 20%, maximum) (Figures 1F, 1G, 1H).

Inhibition of MAPK Pathways and Focal Contact Organization

Figure 5 illustrates variations of VN and VA obtained in 26 hours-serum-starved ROS 17/2.8 in the presence of PD-98059 (50 μM) in unstrained (middle column) and strained (right column) conditions. The long-term effects of the ERK Inhibitor were controlled in unstrained cells over 24 hours, as western blot data indicated progressive dephosphorylation of ERK-2 over a period of eight hours (data not shown). In unstrained cells, PD-98059 initially induced a twofold increase in VN after 1 hour, compared to controls in the absence of inhibitor; VN subsequently decreased and reached control values without inhibitor after six hours (middle column). In strained cells, PD-98059 prevented strain-induced VN variations as a function of time. However, at T24h, VN was higher in strained plus PD-98059 conditions than in the strain only group. PD-98059 tripled VA after one hour compared to controls without inhibitor, then VA decreased between two and three hours and increased again after three hours (middle column). In strain plus PD-98059 conditions (right column), VA initially decreased at T0, then returned to control values. From T2h to T24h, VA was higher than at T0. The VN profile in strained plus PD-98059 conditions did not overlap with that obtained with strain only. In contrast, VA profiles were identical in both strained conditions with and without inhibitor, except that at T24h, VA was higher in strained plus PD-98059 conditions, corresponding to the same level observed in unstrained cells submitted to PD-98059.

Cytoskeletal Organization under Microgravity and Mechanical Stress Conditions

Figure 4 shows representative examples of cytoskeletal structures and vinculin-positive focal contacts under static conditions (BC central line), under microgravity conditions (left line), and under mechanical stress (right line). The first line shows that the number of actin stress fibers is decreased under microgravity conditions and increased under strained conditions, but it should be noted that cell area was reduced under microgravity conditions compared to stretch conditions (Figure 2). The second line shows vinculin staining reflecting the quantification results presented in Figures 1 and 3. The number and area of vinculin-positive contacts increased in cells submitted to mechanical stress. The third line shows vimentin structure that presented a disorganized network under stretch conditions. The same comments can be applied to beta-tubulin staining, as shown in the fourth line. Tubules were completely disorganized under mechanical stress conditions, while the vimentin and tubulin network under microgravity conditions was not significantly different from that observed in BC cells. In summary, the actin network and focal adhesion appeared to be impaired after 12 hours of microgravity, but few effects were detected on the vimentin and tubule network. Conversely, 12 hours after stretch, microtubules were completely disorganized, while stress fibres and the number of focal contacts increased.

DISCUSSION

Few studies have integrated quantitative morphologic data with anchorage-dependent cell type submitted to mechanical stresses. In this study, we present a unique comparison between a mechanical stimulus generating strain at focal adhesion sites and a mechanical stimulus reducing gravitational forces

(microgravity) leading to general relaxation of internal cell tension (10). We demonstrate that mechanotransduction events in osteoblastic cells may be associated with concomitant alterations of structure and function. As the interconnection between the cytoskeleton and the extracellular matrix (ECM) provides an efficient mechanical couple responsible for changes in cell shape, we studied focal adhesion plaques which mediate the cytoskeleton-ECM interactions. These adhesion plaques are considered to be integrative devices for both mechanical signaling and soluble factor-dependent signaling (34). We collected integrin-mediated adhesion data based on detection of vinculin (in primary cells and ROS 17/2.8 cells) at focal adhesion sites by immunostaining to compare focal adhesion adaptation under relaxed or strained conditions.

For strained cells, the kinetics of vinculin-related changes, in both cell types, included an early increase in vinculin spot number (VN) followed by a progressive decrease. When vinculin spot number began to decrease, a sustained increase in vinculin spot area (VA) was seen, that had not returned to baseline values at T24h. It is noteworthy that, at 0.3% and 0.5% deformations, vinculin parameters were completely normal (data not shown), suggesting a sensitivity of adhesion to strain amplitude. These events constituted reorganization, as they did not require vinculin synthesis. This increase in focal contact size could result from either clustering of small, disorganized, and probably less mature contacts, or from formation of new complexes, representing an adaptation to mechanical signals. Clustering probably took place at particular sites of the ventral cell membrane, leading to tethering of the cell to its substrate, while the cell became more contracted. The absence of increased synthesis of vinculin protein and other cytoskeletal proteins (α-actinin and talin) has also been observed in osteoblastic cells submitted to shear stress (25). This last study reported reorganization of stress fibers and concentration of β1-integrin to focal contact sites. Our topographic analysis did not reveal any preferential realignment of vinculin plaques in response to strain, as seen for example in $\alpha_V\beta_3$ plaques of human osteoblasts submitted to 48 hours of cyclic stretch (42). In these last two studies, and in our own study, cell proliferation was increased in response to shear stress or cyclic strain.

For relaxed conditions (i.e., microgravity conditions), we demonstrated that short-term adaptation (24 h) to microgravity was characterized by a sustained decrease of cell area, VN, and VA compared to centrifuge (1 g) cultures or ground control cultures. We have previously demonstrated, after a longer mission, that the antiadhesive effect of microgravity reached a maximum after four days of flight (10). This long-term effect was also characterized by a decrease in cell area, VN, VA, and in the level of phosphorylated proteins present in focal contacts. Focal contact signaling activities were therefore clearly reduced under microgravity conditions. More generally, it is known that microgravity alters microtubules (17) and F-actin integrity [(10) and this study]. Such cytoskeletal alterations could lead to a reduction in cell proliferation (29) and/or an increase in cell apoptosis (30).

Extracellular signal-regulated kinases (ERKs), members of the mitogen-activated protein kinase family, play an important role in the promotion of osteoblast proliferation and differentiation (15). We therefore tested whether the ERK signalling cascade in strained cells was linked to strain-related cell proliferation. We used PD-98059 to induce MEK1/2 inhibition in order to study the relationship between ERK1/2 and cell proliferation. The addition of PD-98059 significantly lowered cell growth under strain and unstrained conditions compared to uninhibited conditions; nevertheless, ERK inhibition did not prevent significant growth of strained cells. This demonstrated that the ERK1/2 pathway is partly required during the strain-induced mitogenic effect. Based on recent studies by Guicheux et al. (35) in MC3T3-E1 cells, we assumed that p38 might be the other MAPK stimulated by mechanical stimulus when ERK activation is inhibited. We also showed that PD-98059 prevented the strain-related decrease in cell area, but had no effect on unstrained cells. In contrast, PD-98059 increased basal levels of both VN and VA in unstrained cells, resulting in

increased focal adhesion. However, for VN, this effect was progressively reduced as a function of time. In strained cells, PD-98059 abolished strain-related fluctuations of VN. Strain alone increased VN more than PD-98059 alone and more than the combination of strain and PD-98059, suggesting that ERK1/2 activation was required for the strain-induced increase in VN. In contrast, PD-98059 did not alter the increase in VA observed in strained cells, suggesting that ERK1/2 tyrosine phosphorylation was not essential for the strain-induced increase in VA. We have therefore demonstrated the presence of a feedback between the formation of vinculin-positive focal contacts and the Ras/ERK pathway and we also provide evidence that vinculin relocation (VN) and clustering (VA) are mediated via different mechanisms. Strain did not require ERK1/2 activation to increase spot surface, but this was not the case for spot number.

Based on the fact that mechanical strain alone, independently of ERKs stimulation, was able to induce cell proliferation and that the kinetic profile of vinculin plaque area was identical in strained cells with or without ERKs inhibitor, it is tempting to speculate that the level of integrin clustering might be a direct regulator of cell proliferation. A clustering level characterized by plaques of at least 0.15 μm^2 (Figure 4) was systematically observed when cell number increased, suggesting that cell proliferation in this configuration is significantly higher than cell death. In contrast, under microgravity conditions, in which the clustering level is characterized by plaques sizes less than 0.05 μm^2, cell number was only maintained under these conditions, suggesting a survival configuration. VA could be proposed as a molecular switch between cell survival or cell proliferation.

It has now been clearly established that integrins functions can constitute a survival factor (11). Experimental studies have shown that clustered integrins at focal contact sites also act as mechanoreceptors (or sensors, or transducers) in a variety of cell types, meaning that molecular connections between integrins and cytoskeletal filaments provide a discrete path for mechanical signal transfer within cells (see 1 for review). Our results, based on the reorganization of vinculin spots in space and time, provide evidence that focal contacts act as mechanoeffectors suggesting that they could be involved in the complex feedback interplay between the cell's cytoskeleton and focal adhesion sites. We showed that, under relaxed conditions, actin stress fibers were confined to the cell periphery, whereas microtubules did not appear to be affected. In contrast, under mechanical stress conditions, actin stress fibers were more numerous and reinforced, and microtubules were clearly depolymerized. Our results demonstrate a continuum of responses from decreased to increased mechanical stresses in actin network and focal contact organization, suggesting that focal adhesion is a key regulator of adaptation to mechanical environments.

Maturation of focal contacts is a complex process depending on the dynamics and stability of actin cables, and both processes are under the control of Rho members of the GTPase family (22, 28). In microgravity, cell adhesion could be restricted to small immature spots. Turnover of focal adhesion sites is negatively correlated with Rho activity (8, 43). An increase in focal adhesion turnover in relaxed ROS 17/2.8 cells could be correlated to a permanent decrease in GTPase activities leading to decreased clustering of focal contacts. It is now clear that the release of focal adhesion sites is controlled by microtubules. Microtubule targeting of substrate contacts promotes their relaxation and dissociation (13, 14). In this study, the fact that the microtubule network is not affected by microgravity indicated that the microtubule network is still compatible with tubules' relaxing activity on focal adhesion. Interestingly, the disruption of tubules under strain conditions associated with the formation of large stress fibers could indicate that the balance between formation and release of focal contacts under conditions of mechanical stress is in favor of formation of focal contacts, as tubules are no longer able to tag focal contacts. We propose that a decrease in mechanical strain induces a reduction in actin-myosin activity, leading to a reduction in focal contact maturation (as determined by the size of clusters) and that, at the same time, the microtubule contact-relaxing activity is maintained. The long-term adaptation to this

situation might be a dramatic reduction in cell adhesion leading to apoptosis. In the opposite case, cells submitted to increased mechanical strain present increased stress fiber formation as well as focal contact formation and maturation, leading to formation of large signalling complexes able to support mitogenic responses in synergy with growth factors (44). The observed depolymerization of tubules after 12 hours of stretch might also induce formation of new focal contacts.

It is difficult to manipulate the size of focal contacts, except by microtubule treatment (14), but this long-term treatment could alter the cell's proliferative capacities. Modulation of cell shape is easier to control. Traditional approaches designed to modulate cell shape, either by attaching suspended cells to microbeads of different sizes or by plating cells on substrates coated with different densities of matrices, suggested that cell shape may play an important role in control of growth. Progressively restricting endothelial cell extension by culturing cells on smaller and smaller micropatterned adhesive substrate islands regulates a transition from growth to apoptosis on a single continuum of cell spreading, thus confirming the central role of cell shape in cell growth (6). However, Schwartz et al. (32) showed that hepatocyte cell attachment to insoluble fibronectin clusters and immobilized integrins $\alpha 5\beta 1$, independent of cell shape, activates a signaling pathway involved in cell growth. The well accepted idea that anchorage-dependent cell spreading is a prerequisite for cells to proliferate is therefore contradicted by this last result and by our data suggesting that increased focal contact clustering allows maintenance of growth, even without cell spreading.

In conclusion, we describe topographic vinculin-positive adhesion changes in response to two opposing mechanical stimuli. We demonstrate that adaptation of focal adhesion is intimately related to the mechanical environment and that focal adhesion cluster size is a discriminant parameter between mitogenic and nonmitogenic mechanical regimens. Focal contacts appear to be mechanoeffectors controlling the complex interplay between mechanical and chemical events in the cell and its membrane. Maturation of focal clusters could be linked to cytoskeletal integrity as modulated by external mechanical stress and can be proposed as a molecular switch between cell survival or cell proliferation.

ACKNOWLEDGMENTS

This work was supported by grants from ERISTO (European Research In Space and Terrestrial Osteoporosis), INSERM (n# 4M111C), and the Région Rhône-Alpes. OA was funded by FRM (Fondation pour la Recherche Medicale).

REFERENCES

1. Alenghat FJ, Ingber DE (2002). Mechanotransduction: All signals point to cytoskeleton, matrix, and integrins. *Sci STKE* 119: PE6.
2. Brighton CT, Sennet BJ, Farmer JC, Iannoti JP, Hansen CA, Williams JL, Williamson J (1992). The inositol phosphate pathway as a mediator in the proliferative response of rat calvarial bone cells to cyclical biaxial mechanical strain. *J Orthop Res* 10: 385–393.
3. Carvalho RS, Schaffer JL, Gerstenfeld LC (1998). Osteoblasts induce osteopontin expression in response to attachment on fibronectin: Demonstration of a common role for integrin receptors in the signal transduction processes of cell attachment and mechanical stimulation. *J Cell Biochem* 70: 376–390.
4. Carvalho R, Scott JE, Suga DM, Yen EK (1994). Stimulation of signal transduction pathways in osteoblasts by mechanical strain potentiated by parathyroid hormone. *J Bone Miner Res* 9: 999–1010.
5. Cary LA, Han DC, Guan JL (1999). Integrin-mediated signal transduction pathways. *Histol Histopathol* 14: 1001–1009.
6. Chen CS, Mrksich M, Huang S, Whitesides GM, Ingber DE (1998). Micropatterned surfaces for control of cell shape, position, and function. *Biotechnol Prog* 14: 356–363.
7. Chess PR, Toia L, Finkelstein JN (2000). Mechanical strain-induced proliferation and signaling in pulmonary epithelial H441 cells. *Am J Physiol Lung Cell Mol Physiol* 279: L43–L51.
8. Defilippi P, Venturino M, Gulino D, Duperray A, Boquet P, Fiorentini C, Volpe G, Palmieri M, Silengo L, Tarone G (1997). Dissection of pathways implicated in integrin-mediated actin cytoskeleton assembly. Involvement of protein kinase C, Rho GTPase and tyrosine phosphorylation. *J Biol Chem* 272: 21726–21734.
9. Guignandon A, Genty C, Vico L, Lafage-Proust MH, Palle S, Alexandre C (1997). Demonstration of feasibility of automated osteoblastic line culture in space flight. *Bone* 20: 109–116.
10. Guignandon A, Lafage-Proust MH, Usson Y, Laroche N, Caillot-Augusseau A, Alexandre C, Vico L (2001). Cell cycling determines integrin-mediated adhesion in osteoblastic ROS 17/2.8 cells exposed to space-related conditions. *FASEB J* 15: 2036–2038.

11. Hirsch E, Barberis L, Brancaccio M, Azzolino O, Xu D, Kyriakis JM, Silengo L, Giancotti FG, Tarone G, Fassler R, Altruda F (2002). Defective Rac-mediated proliferation and survival after targeted mutation of the {beta}1 integrin cytodomain. *J Cell Biol* 157: 481–492.
12. Ilic D, Damsky CH, Yamamoto T (1997). Focal adhesion kinase: At the crossroads of signal transduction. *J Cell Sci* 110: 401–407.
13. Kaverina I, Krylyshkina O, Small JV (1999). Microtubule targeting of substrate contacts promotes their relaxation and dissociation. *J Cell Biol* 146: 1033–1044.
14. Krylyshkina O, Kaverina I, Kranewitter W, Steffen W, Alonso MC, Cross RA, Small JV (2002). Modulation of substrate adhesion dynamics via microtubule targeting requires kinesin-1. *J Cell Biol* 156: 349–359.
15. Lai CF, Chaudhary L, Fausto A, Halstead LR, Ory DS, Avioli LV, Cheng SL (2001). Erk is essential for growth, differentiation, integrin expression, and cell function in human osteoblastic cells. *J Biol Chem* 276: 14443–14450.
16. Lavoie JN, L'Allemain G, Brunet A, Muller R, Pouyssegur J (1996). Cyclin d1 expression is regulated positively by the p42/p44MAPK and negatively by the p38/HOG MAPK pathway. *J Biol Chem* 271: 20608–20616.
17. Lewis ML, Reynolds JL, Cubano LA, Hatton JP, Lawless BD, Piepmeier EH (1998). Spaceflight alters microtubules and increases apoptosis in human lymphocytes (Jurkat). *FASEB J* 12: 1007–1018.
18. Mainly B (1986) *Multivariate Statistical Analysis, A primer*. Chapman & Hall Ed, London, New-York, pp. 86–99.
19. Meazzini MC, Toma CD, Schaffer JL, Gray ML, Gerstenfeld LC (1998). Osteoblast cytoskeletal modulation in response to mechanical strain in vitro. *J Orthop Res* 16: 170–180.
20. Miyamoto S, Teramoto H, Coso O, Gutking J, Burbelo P, Akiyama S, Yamada K (1995). Integrin function: Molecular hierarchies of cytoskeletal and signaling molecules. *J Cell Biol* 131: 791–805.
21. Nobes CD, Hall A (1995). Rho, rac, and cdc42 GTPases regulate the assembly of multimolecular focal complexes associated with actin stress fibers, lamellipodia, and filopodia. *Cell* 81: 53–62.
22. Nobes CD, Hall A (1999). Rho GTPases control polarity, protrusion, and adhesion during cell movement. *J Cell Biol* 144: 1235–1244.
23. Nomura S, Takano-Yamamoto T (2000). Molecular events caused by mechanical stress in bone. *Matrix Biol* 19: 91–96.
24. Oxlund H, Andersen NB, Ortoft G, Orskov H, Andreassen TT (1998). Growth hormone and mild exercise in combination markedly enhance cortical bone formation and strength in old rats. *Endocrinol* 139: 1899–1904.
25. Pavalko FM, Chen NX, Turner CH, Burr DB, Atkinson S, Hsieh YF, Qiu J, Duncan RL (1998). Fluid shear-induced mechanical signaling in MC3T3-E1, osteoblasts requires cytoskeleton-integrin interactions. *Am J Physiol* 275: C1591–C1601.
26. Pommerenke H, Schreiber E, Durr F, Nebe B, Hahnel C, Moller W, Rychly J (1996). Stimulation of integrin receptors using a magnetic drag force device induces an intracellular free calcium response. *Eur J Cell Biol* 70: 157–164.
27. Richardson A, Parsons JT (1995). Signal transduction through integrins: A central role for focal adhesion kinase? *BioEssays* 17: 229–236.
28. Ridley AJ, Hall A (1992). The small GTP-binding protein Rho regulates the assembly of focal adhesions and actin stress fibers in response to growth factors. *Cell* 70: 389–399.
29. Rucci N, Migliaccio S, Zani BM, Taranta A, Teti A (2002). Characterization of the osteoblast-like cell phenotype under microgravity conditions in the NASA-approved rotating wall vessel bioreactor (RWV). *J Cell Biochem* 85: 167–179.
30. Sarkar D, Nagaya T, Koga K, Nomura Y, Gruener R, Seo H (2000). Culture in vector-averaged gravity under clinostat rotation results in apoptosis of osteoblastic ROS 17/2.8 cells. *J Bone Miner Res* 15: 489–498.
31. Schwartz MA (1997). Integrins, oncogenes, and anchorage independence. *J Cell Biol* 139: 575–578.
32. Schwartz MA, Lechene C, Ingber DE (1991). Insoluble fibronectin activates the Na/H antiporter by clustering and immobilizing integrin alpha 5 beta 1, independent of cell shape. *Proc Natl Acad Sci USA* 88: 7849–7853.
33. Schlaepfer DD, Hauck CR, Sieg DJ (1999). Signaling through focal adhesion kinase. *Prog Biophys Mol Biol* 71: 435–478.
34. Shyy JY, Chien S (1997). Role of integrins in cellular responses to mechanical stress and adhesion. *Curr Opin Cell Biol* 9: 707–713.
35. Suzuki A, Guicheux J, Palmer G, Miura Y, Oiso Y, Bonjour JP, Caverzasio J (2002). Evidence for a role of p38 MAP kinase in expression of alkaline phosphatase during osteoblastic cell differentiation. *Bone* 30: 91–99.
36. Takahashi M, Ishida T, Traub O, Corson MA, Berk BC (1997). Mechanotransduction in endothelial cells: Temporal signaling events in response to shear stress. *J Vasc Res* 34: 212–219.
37. Tatsumi R, Sheehan SM, Iwasaki H, Hattori A, Allen RE (2001). Mechanical stretch induces activation of skeletal muscle satellite cells in vitro. *Exp Cell Res* 267: 107–114.
38. Turner CH, Pavalko FM (1998). Mechanotransduction and functional response of the skeleton to physical stress: The mechanisms and mechanics of bone adaptation. *J Orthop Sci* 3: 346–355.
39. Usson Y, Guignandon A, Laroche N, Lafage-Proust MH, Vico L (1997). Quantitation of cell-matrix adhesion using confocal image analysis of focal contact associated proteins and interference reflection microscopy. *Cytometry* 28: 298–304.
40. Vico L, Collet P, Guignandon A, Lafage-Proust MH, Thomas T, Rehaillia M, Alexandre C (2000). Effects of long-term microgravity exposure on cancellous and cortical weight-bearing bones of cosmonauts. *Lancet* 355: 1607–1611.
41. Wang N, Naruse K, Stamenovic D, Fredberg JJ, Mijailovich SM, Tolic-Norrelykke IM, Polte T, Mannix R, Ingber DE (2001). Mechanical behavior in living cells consistent with the tensegrity model. *Proc Natl Acad Sci USA* 98: 7765–7770.
42. Wozniak M, Fausto A, Carron CP, Meyer DM, Hruska KA (2000). Mechanically strained cells of the osteoblast lineage organize their extracellular matrix through unique sites of alpha v beta3-integrin expression. *J Bone Miner Res* 15: 1731–1745.
43. Xiang-Dong R, Kiosses W, Sieg D, Otey C, Schlaepfer D, Schwartz M (2000). Focal adhesion kinase suppresses Rho activity to promote focal adhesion turnover. *J Cell Sci* 113: 3673–3678.
44. Yamada KM, Even-Ram S (2002). Integrin regulation of growth factor receptors. *Nat Cell Biol* 4: E75–E76.
45. Zou Y, Hu Y, Metzler B, Xu Q (1998). Signal transduction in arteriosclerosis: Mechanical stress-activated MAP kinases in vascular smooth muscle cells. *Int J Mol Med* 1: 827–834.